analytical chemistry

pubs.acs.org/ac Article

Voltammetric Approach for Characterizing the Biophysical and Chemical Functionality of Human Induced Pluripotent Stem Cell-Derived Serotonin Neurons

Jordan Holmes,[¶] Thorsten Lau,[¶] Rachel Saylor, Nadine Fernández-Novel, Melinda Hersey, Deanna Keen, Lena Hampel, Sandra Horschitz, Julia Ladewig, Brenna Parke, Michael C. Reed, H. Frederik Nijhout, Janet Best, Philipp Koch,* and Parastoo Hashemi*

Cite This: https://doi.org/10.1021/acs.analchem.1c05082 Read Online

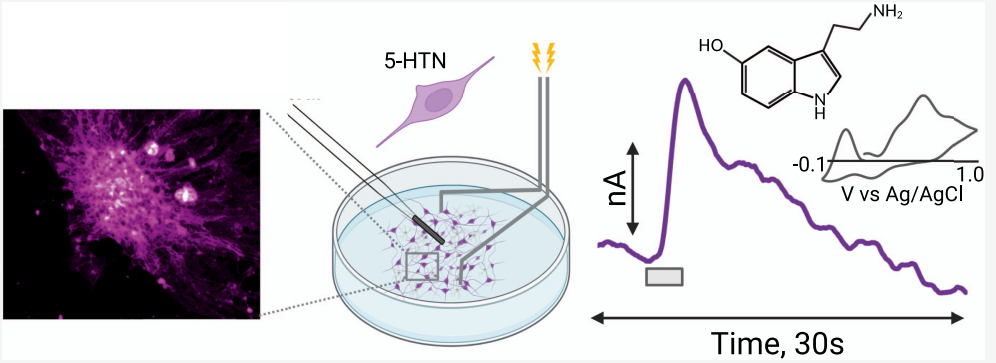

ABSTRACT: Depression is quickly becoming one of the world's most pressing public health crises, and there is an urgent need for better diagnostics and therapeutics. Behavioral models in animals and humans have not adequately addressed the diagnosis and treatment of depression, and biomarkers of mental illnesses remain ill-defined. It has been very difficult to identify biomarkers of depression because of *in vivo* measurement challenges. While our group has made important strides in developing *in vivo* tools to measure such biomarkers (e.g., serotonin) in mice using voltammetry, these tools cannot be easily applied for depression diagnosis and drug screening in humans due to the inaccessibility of the human brain. In this work, we take a chemical approach, *ex vivo*, to introduce a human-derived system to investigate brain serotonin. We utilize human induced pluripotent stem cells differentiated into serotonin neurons and establish a new *ex vivo* model of real-time serotonin neurotransmission measurements. We show that evoked serotonin release responds to stimulation intensity and tryptophan preloading, and that serotonin release and reuptake kinetics resemble those found *in vivo* in rodents. Finally, after selective serotonin reuptake inhibitor (SSRI) exposure, we find dose-dependent internalization of the serotonin reuptake transporters (a signature of the *in vivo* response to SSRI). Our new human-derived chemical model has great potential to provide an *ex vivo* chemical platform as a translational tool for *in vivo* neuropsychopharmacology.

INTRODUCTION

Depression is already one of the world's most pressing health issues, and projections are that in a post-COVID era, this disorder will account for unprecedented burdens.[1,2] Current diagnostics and therapeutics are not based on chemical markers (because the chemistry of depression remains poorly understood), and thus fall short for many patients.[3,4] Taken together, these facets constitute an urgent need for more accurate, personalized diagnostics and therapeutics. In response to this, our group has, over the past decade, developed cutting-edge chemical tools for defining serotonin (analyte of interest in the pathology of depression) signaling in real time *in vivo*. Using these tools, we have defined several important aspects of *in vivo* serotonin neurochemistry.[5−10] These previous studies facilitated an understanding of how depression comorbidities influence extracellular serotonin and the direct and indirect actions of antidepressants on the serotonin system,[11,12] allowing us to improve the chemical efficacy of the common therapies.[11]

To translate this work to humans for diagnostic/therapeutic purposes, we sought a model system outside of the brain that is representative of human physiology. The introduction of human induced pluripotent stem cells (iPS cells) to the scientific

Received: November 23, 2021
Accepted: April 27, 2022

https://doi.org/10.1021/acs.analchem.1c05082
Anal. Chem. XXXX, XXX, XXX−XXX

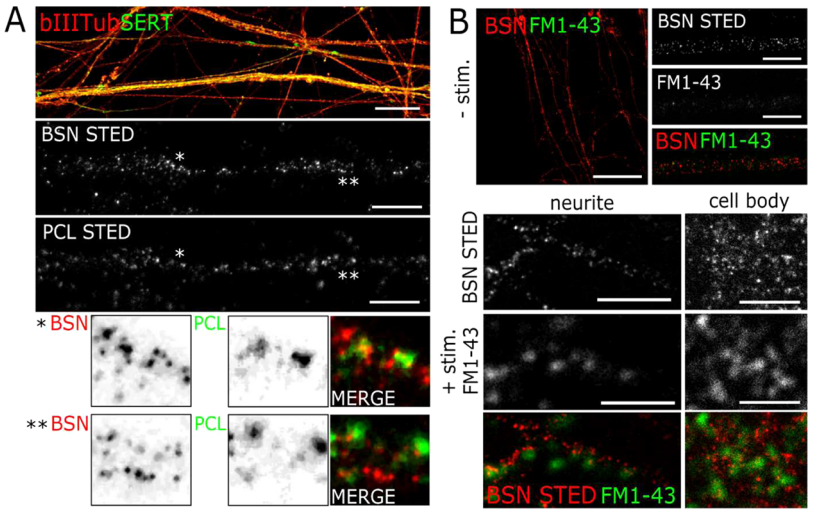

Figure 1. Visualization of serotonin release. (A) Localization of the presynaptic scaffold proteins Bassoon and Piccolo on the neurites of 5-HTNs. Top: the exemplary image of the neuronal network identified by betaIII-Tubulin (bIIITub) and SERT immunostaining; scale bar 25 μm. STED microscopy revealed that the presynaptic markers bassoon and piccolo are expressed on SERT-positive neurites (SERT co-staining for STED images is shown in Figure S3A). Scale bars: 2 μm. * and ** show randomly selected areas with overlapping BSN and PCL signals. (B) Uptake of the membrane dye FM1-43 is triggered by electrical stimulation of the neurons. Without stimulation (-stim), no FM1-43 uptake into BSN-positive structures is observed. Electrical stimulation (+stim) induced FM1-43 uptake at BSN-positive active zones on neurites and cell bodies. Scale bars: 25 μm, STED images: 2 μm.

community has created a new approach to establishing human *in vitro* disease models, e.g., the ability to investigate patient-specific genetic backgrounds.[13−15] Recently, efficient differentiation protocols for serotonergic neurons (5-HTNs) from human iPS cells have been developed.[16] These iPS cell-derived neurons have been shown to successfully integrate into neuronal networks after transplantation into the rodent brain and display outgrowth of axonal projections to the cerebellum and spinal cord. This observation implies that 5-HTNs exhibit morphological features compatible with serotonin neurons[17] and suggest that human iPS cell-derived 5-HTNs can be valuable as an *ex vivo* model. To this end, we are interested in ascertaining whether these models maintain the serotonin chemical functionality and response to antidepressants that we observe *in vivo* with voltammetry.

In this work, we establish a new *ex vivo* model of real-time serotonin measurements from human iPS cell-derived 5-HTNs. We verify that these neurons are chemically functional by developing a voltammetric model, including optimizing detection medium and stimulation parameters. Excitingly, we show that evoked serotonin release responds to stimulation intensity and tryptophan preloading. Serotonin release and reuptake kinetics resemble those found *in vivo* in rodents such that *in vitro* data could be fitted well with a computational model generated from *in vivo* data that incorporates multiple reuptake mechanisms and autoreceptor control. Finally, following administration of the selective serotonin reuptake inhibitor (SSRI), escitalopram (ESCIT), we chemically and microscopically show dose-dependent internalization of the serotonin transporters (SERTs) (a key feature of the *in vivo* response to SSRI). Our new human-derived model has great potential to provide an *in vitro* chemical platform as a translational tool for advanced and personalized diagnostic neuropsychopharmacology.

■ MATERIALS AND METHODS

Detailed information about experimental design can be found in Supporting Information (full methods). 5-HTNs were generated using an iPS cell line generated in the Koch laboratory. Generation comprised four stages, each consisting of cultivation in defined differentiation media for neuronal induction, ventralization, promotion of serotonergic progenitors, and terminal differentiation. Differentiation started from a nearly confluent culture of iPS cells. If cells reached confluence again, they were mechanically passaged 1:3 and replated. Prior to terminal differentiation, cells were split on glass coverslips for fast scan cyclic voltammetry (FSCV) and immunofluorescence analysis or in 3.5 cm Ibidi imaging chambers (Ibidi, Munich, Germany) for live-cell imaging experiments. Microscopy analyses were performed using a Leica THUNDER Imaging System (Leica Microsystems, Wetzlar, Germany) or Cell Discoverer 7 Imaging System (Zeiss, Jena, Germany) for conventional fluorescence microscopy, a Leica TCS SP5 (Leica Microsystems, Mannheim, Germany) for confocal laser microscopy and live-cell experiments, and a Steadycon microscope setup for STED microscopy (Abberior Instruments, Göttingen, Germany).

Carbon fiber microelectrode (CFM) fabrication and FSCV data acquisition/analysis were described previously.[6,8] Coverslips containing neuronal cell clusters were placed into a 35 mm low wall imaging dish (Ibidi GmbH, Martinsried, Germany) and were covered with a solution containing 2.5 mM glucose in HEPES buffer, a common pH balancing molecule in cell media. This dish was placed into a plastic holder covered with aluminum foil connected to the ground, acting as a Faraday cage. A Nafion-coated CFM and stimulation electrode were positioned into the cells, and a Ag/AgCl reference (A-M Systems, Sequim, WA) electrode was placed in the dish under a Leica DM IL inverted microscope. Electrical stimulation was applied to stimulation pins 1 mm apart.

In vivo FSCV experiments were approved by the Ethical Committee of Animal Research at the University of South Carolina and performed by administering 25% w/v urethane at 7 μL/g of body weight via intraperitoneal (*i.p.*) injection to mice. The anesthetized mice were placed into a stereotaxic instrument (David Kopf Instruments, Tujunga, CA). FSCV was performed

https://doi.org/10.1021/acs.analchem.1c05082
Anal. Chem. XXXX, XXX, XXX−XXX

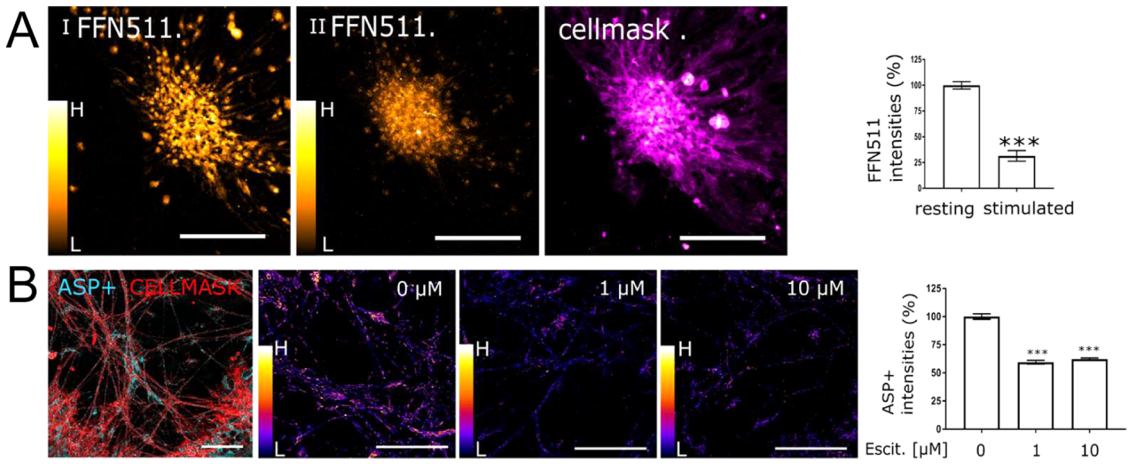

Figure 2. Visualization of serotonin uptake: (A) Evoked false neurotransmitter (FFN511) release. Images show an exemplary neuronal cluster (i) before and (ii) after stimulation. Cellmask staining was applied to determine ROI for quantification of FFN511 release. The Orange Hot LUT bar (NIH ImageJ) indicates pixel intensities. Scale bars: 100 μm. (B) Representative projection of a confocal z-stack, scale bar: 50 μm. Cellmask staining was applied to select ROI for quantification of ASP+ uptake. Randomly selected z-projections show ASP fluorescence intensities of the control and ESCIT-treated neurons. Fire LUT bar (NIH ImageJ) displays pixel intensities; scale bars: 50 μm. Statistical analysis of microscopy data for FFN511 release and ASP+ uptake is shown in the respective graphs (for each $n = 3$ independent experiments; ***, $p < 0.01$).

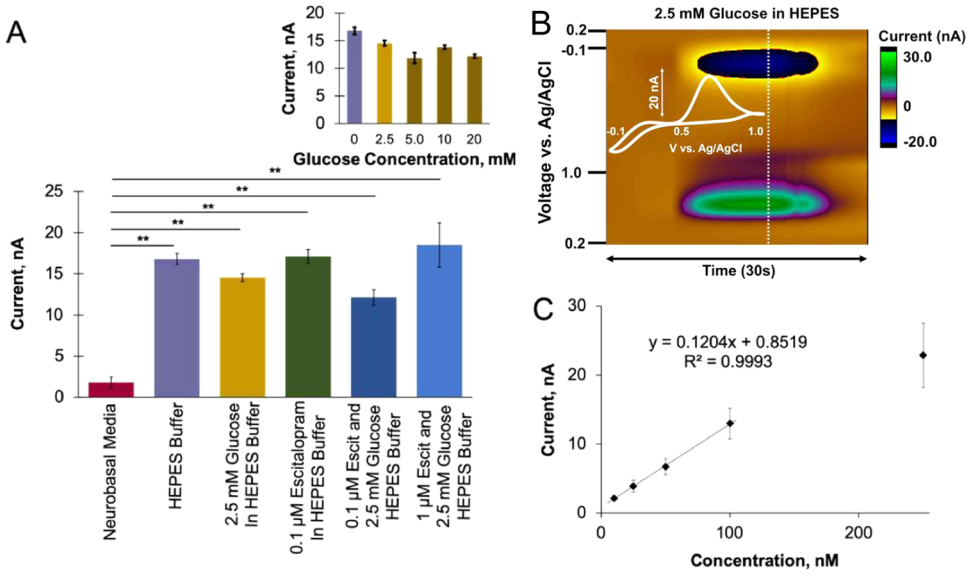

Figure 3. FSCV Electrolytic Buffer Optimization. (A) Comparisons of electrolytic media for FSCV analysis, including neurobasal media, HEPES, glucose, and ESCIT (** $p < 0.005$). The inset shows various concentrations of glucose added to the media (not significant). (B) Representative color plot for selected buffer composition (2.5 mM glucose in HEPES) with CV inset. Briefly, 250 nM serotonin was used for all medium optimization experiments. (C) Calibration curve; concentration of serotonin in nM vs current response ($n = 5$) ± SEM.

by lowering CFMs into the CA2 region of the hippocampus while stimulating the medial forebrain bundle in 6- to 12-week-old C57BL/6 mice (Jackson Laboratory, Bar Harbor, ME). Exclusion criteria and more detailed information on FSCV and animal experiments are presented in the Supporting Information.

RESULTS

Verification of Serotonin Release and Reuptake Sites in Human iPS Cell-Derived Serotonergic Neurons. We generated serotonergic neurons according to a protocol by Lu and colleagues[16] and characterized the cells in depth (see Supporting Information: Generation of Serotonergic Neurons from Human Induced Pluripotent Stem Cells). We found the presynaptic active zone scaffolding proteins Piccolo and Bassoon, required to establish and maintain the presynapse,[18] localized in the cell bodies and neurites of the 5-HTNs expressing SERT (Figures 1A and S3A). Electrical stimulation caused uptake of the dye FM1-43 (shown to associate with synaptic vesicles) into vesicle-like structures, which were successfully counterstained for the presynaptic scaffolding protein Bassoon (Figure 1B). This indicates that Bassoon and Piccolo maintain active zones not exclusively at nerve terminals and that neurotransmitter release may occur at extrasynaptic release sites, as typically observed in serotonergic neurons *in vivo*.

To demonstrate that electrical stimulation evokes vesicular release of monoamines, 5-HTNs were loaded with a fluorescent false neurotransmitter, FFN511, which is selectively transported into monoamine-containing neurotransmitter vesicles by

https://doi.org/10.1021/acs.analchem.1c05082
Anal. Chem. XXXX, XXX, XXX−XXX

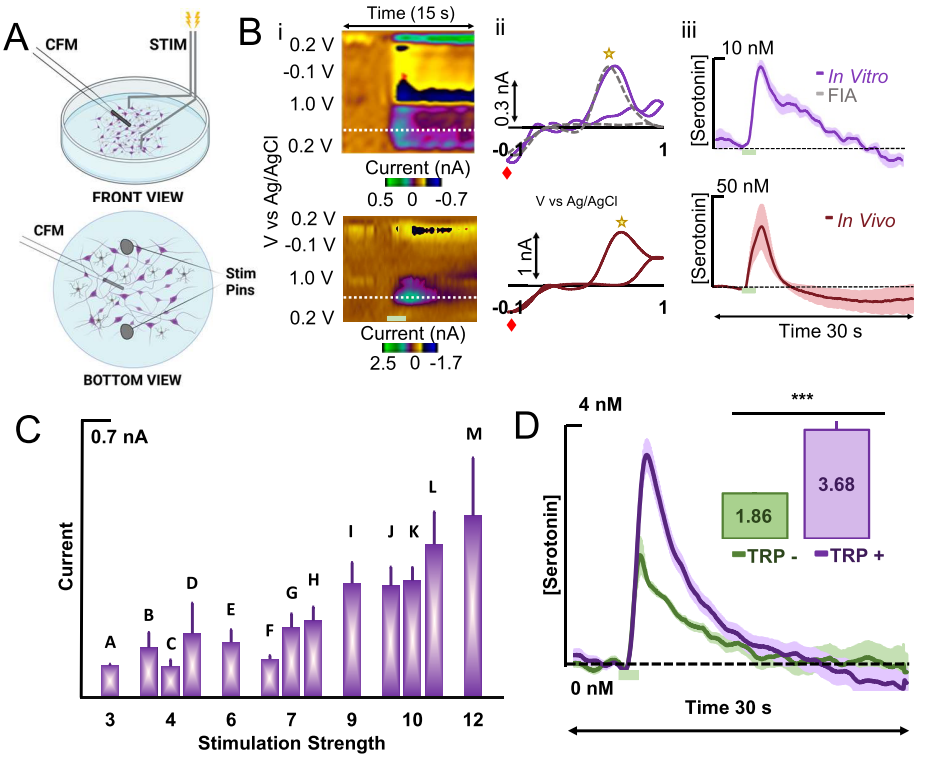

Figure 4. FSCV Analysis of 5-HTNs. (A) Schematic representation of the experimental setup: the CFM was lowered onto the cell cluster, and two stimulation pins (STIM) were used for electrical stimulation. Both panels represent the same experimental setup from different viewpoints (frontal and from underneath the dish). (B) *In vivo* (red), *in vitro* (purple), and serotonin in a flow injection analysis system (FIA) (gray). FSCV (i) color plots, (ii) CVs, and (iii) concentration vs time traces. (C) FSCV current response with respect to stimulation intensity, a function of stimulation amplitude, frequency, and number of pulses. (D) FSCV concentration vs time traces collected following the addition or omission of tryptophan (TRP) to the cellular media 24 h before the analysis. Release amplitude averages are in the inset, showing a significant increase in release (***, $p < 0.001$) following the addition of TRP.

vesicular monoamine transporter 2 (VMAT2) (Figures 2A and S3B). In line with the observation for uptake of the FM1-43 dye into vesicle pools at extrasynaptic release sites, electrical stimulation caused significant depletion of FFN511 fluorescence on the cell bodies and neurites of 5-HTNs. As a result of electrically evoked FFN511 release, intensity levels dropped from 26.31 ± 8.88 to 7.74 ± 1.28 ($p = 0.0399$; $n = 3$ independent experiments (Figure 2A)).

Extrasynaptic release requires the availability of functional, cell surface-located SERTs to reuptake serotonin. To visualize the uptake capacity of such transporters, we employed the fluorescent monoamine transporter substrate ASP+.[19] After uptake, signals for ASP+, which localize to mitochondria, were retrieved from neurites and cell bodies (Figure 2B). Quantitative confocal laser scanning microscopy was used to determine how SERTs participate in ASP+ uptake (Figure 2B). To this end, neurons were treated with 1 and 10 μM of ESCIT to inhibit SERT function. The analysis shows that both doses of ESCIT significantly decreased ASP+ uptake to 59.6 ± 1.6% and 62.2 ± 1.1%, respectively, of the control values (Figure 2B).

Together, our microscopy data indicate that the neuronal cultures have the machinery for serotonin release and reuptake.

Real-Time Serotonin Release and Reuptake in 5-HTNs. Cell culture media consists of a suite of growth factors, amino acids, vitamins, and nutrients that can lead to the biofouling of the carbon surface. In Figure 3, the current response of 250 nM serotonin in standard neurobasal cell culture media is shown in the histogram bar in red. This response is compared to a response in HEPES alone (purple), glucose in HEPES (yellow), ESCIT in HEPES (green), and combinations of glucose and ESCIT in HEPES (light and dark blue). The signal response ($p < 0.005$) in the neurobasal media with respect to each HEPES-based solution is significantly decreased. The addition of glucose and ESCIT does not significantly affect the voltammetric signal response at the concentrations used; therefore, we utilized 2.5 mM glucose in HEPES as our test solution. Figure 3B is a representative color plot, and the inset is the cyclic voltammogram (CV) of serotonin (250 nM). Figure 3C is the calibration for serotonin (10, 25, 50, 100, and 250 nM). In this medium, the linear portion is fitted with a regression model and the limit of detection is 3.43 nM.

We applied FSCV in this optimized media to the 5-HTN cultures. A CFM was positioned in a neuronal cluster enveloped by two stimulation pins (Figure 4A, front and bottom view). Figure 4Bi shows representative color plots with serotonin oxidation and reduction events. Figure 4Bii shows an *in vitro* CV (purple), a serotonin CV taken in a flow injection system (gray), normalized to maximum current, and an *in vivo* (mouse hippocampus) CV (red). Serotonin oxidation is at 0.7 V (star), and reduction is at 0 V (diamond). Additional peaks are likely due to capacitive current because of the low Faradaic currents we are measuring. The slight shift in oxidation *in vivo* is likely due to the ionic microenvironment of the reference electrode changing the chloride equilibrium.[20] Concentration vs time traces, averaged from 4 stimulations in one cell preparation or one animal (*in vivo*), are shown in Figure 4Biii, extrapolated from the horizontal lines in the color plots. Serotonin release

https://doi.org/10.1021/acs.analchem.1c05082
Anal. Chem. XXXX, XXX, XXX−XXX

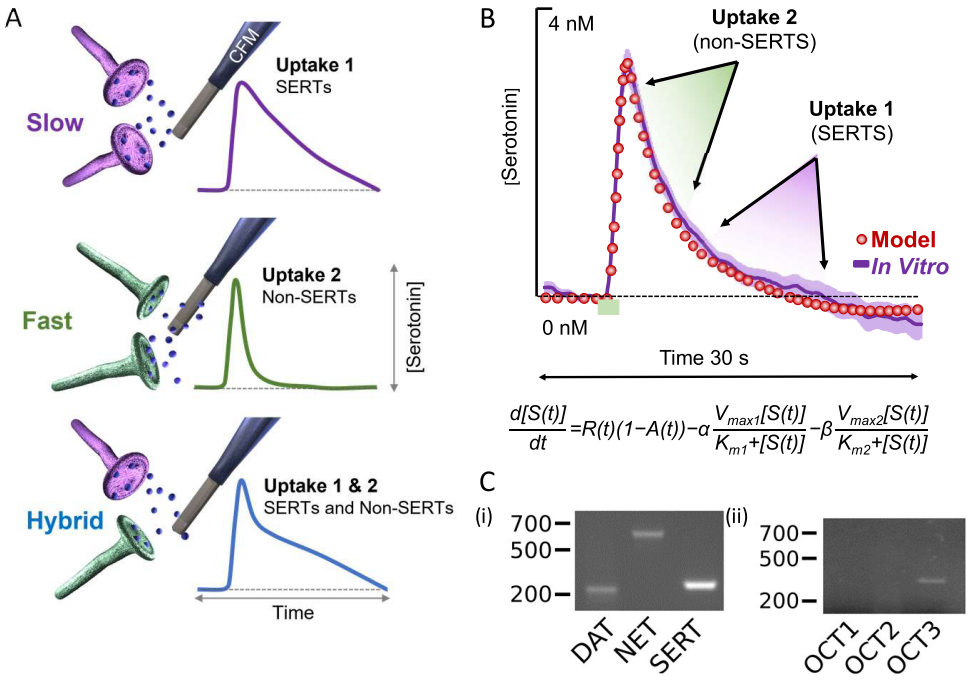

Figure 5. Evidence of Multiple Reuptake Mechanisms. (A) Schematic diagram of two reuptake mechanisms originating from multiple transporters (SERTs and non-SERTs). The effects of the presence of each transporter group on FSCV data are shown on the right, labeled fast (non-SERTs), slow (SERTs), and hybrid (a combination of SERTs and non-SERTs). (B) Representative FSCV current vs time trace collected from the control 5-HTNs (purple) (n = 10 independent experiments), and the dotted curve predicted by the mathematical model (red). The components of the reuptake trace Uptake 1 (purple) and Uptake 2 (green) are highlighted. The equation, previously described by Wood et al.,[7] describing the contributions of each reuptake mechanism toward the FSCV reuptake trace is given below. (C) PCR profile of 5-HTN cultures for monoamine transporters: examples for a (i) differentiation in which DAT, NET, and SERT mRNA are detected, and (ii) in all differentiations made, OCT3 mRNA was detected but not the transcripts for OCT1 nor OCT2.

from the cells was lower than serotonin release *in vivo* in mice (7.48 ± 0.63 nM in cells vs 35.39 ± 13.18 *in vivo*, respectively).

In 3 preparations, stimulation parameters (frequency, amplitude, and pulse number) were applied in strategic combinations, labeled A−M in Figure 4C, and arbitrarily assigned numerical values of 1−4, and these values were added together to reach a sum (3−12) representing the overall stimulation strength (Table S2), which dictated the amplitude of the release. Serotonin release was also dependent on tryptophan (TRP) loading. TRP was added to the culture medium 24 h before analysis, resulting in the purple concentration vs time trace (TRP+) as shown in Figure 4D. The addition of TRP increased the release event amplitude by 97.8% (p = 0.00069).

In Figure 4D, stimulation is denoted by a green bar under the plots. After stimulation, there is rapid serotonin clearance, indicating active reuptake as seen *in vivo*.[10] In prior work, we developed a mathematical model to fit the *in vivo* experimental data as a function of Uptake 1 and Uptake 2 (Figure 5A; see the Discussion section for explanation).[10] The equation we previously developed is shown in Figure 5B; here, the rate of change in serotonin is expressed by serotonin release (R(t)), offset by an autoreceptor term (1-A(t)) and two reuptake mechanisms are given by two Michaelis−Menten terms, preceded by two coefficients (α and β). We found that all *in vivo* signals comprised two reuptake mechanisms to differing degrees by fitting the data with this equation and adjusting the coefficients α and β to account for the difference in local cytoarchitecture.[5,10] Here, we modeled the curves from the 5-HTNs in a similar manner, accounting for TRP loading (Figures 4D and S4); the model fit is shown by the dotted trace in Figure 5B, superimposed over the experimental data. As we previously found *in vivo*, serotonin release from 5-HTNs followed serotonin reuptake characterized by the hybrid model of Uptake 1 and Uptake 2. To confirm that Uptake 2 transporters are present in our cultures, we performed a real-time polymerase chain reaction (RT-PCR) analysis. In addition to SERT, we detected NETs and DATs, as well as OCT3, but not OCT1 nor OCT2 (Figure 5C).

SSRI-Induced Internalization of SERTs in 5-HTNs. We previously observed SSRI-induced SERT internalization in a murine *in vitro* model of serotonin neurons[21] and asked here whether this phenomenon holds for human 5-HTNs. Immunostaining for cell surface-localized SERT shown in Figure 6A revealed signals along the neurites and soma of 5-HTNs. We exposed independent cultures to different concentrations of ESCIT (0.1, 0.5, and 1 μM) and quantified extracellular SERTs after 2 h (Figures 6B and S5). Treatment with 0.1 μM ESCIT caused reduced fluorescence intensity (81.90 ± 7.65%, p = 0.0221), indicating significant SERT internalization. This internalization was dose-dependent (49.58 ± 3.90 and 51.63 ± 4.01%, respectively, for 0.5 and 1 μM ESCIT, compared to the control 5-HTNs, $p < 0.0001$ for both treatments).

As shown in Figure 6C, the three ESCIT concentrations were added to separate preparations. The FSCV traces for the control and 2 h after-ESCIT are shown. Serotonin reuptake decreased after 2 h for all doses of ESCIT, with the majority of the drug's effect on Uptake 1. We mathematically modeled this data and show the model fit *via* the dotted trace. To create these fits, we first chose parameters so that the computed extracellular serotonin curve matched the control values and then modified the coefficients to account for uptake inhibition. Uptake curves

https://doi.org/10.1021/acs.analchem.1c05082
Anal. Chem. XXXX, XXX, XXX−XXX

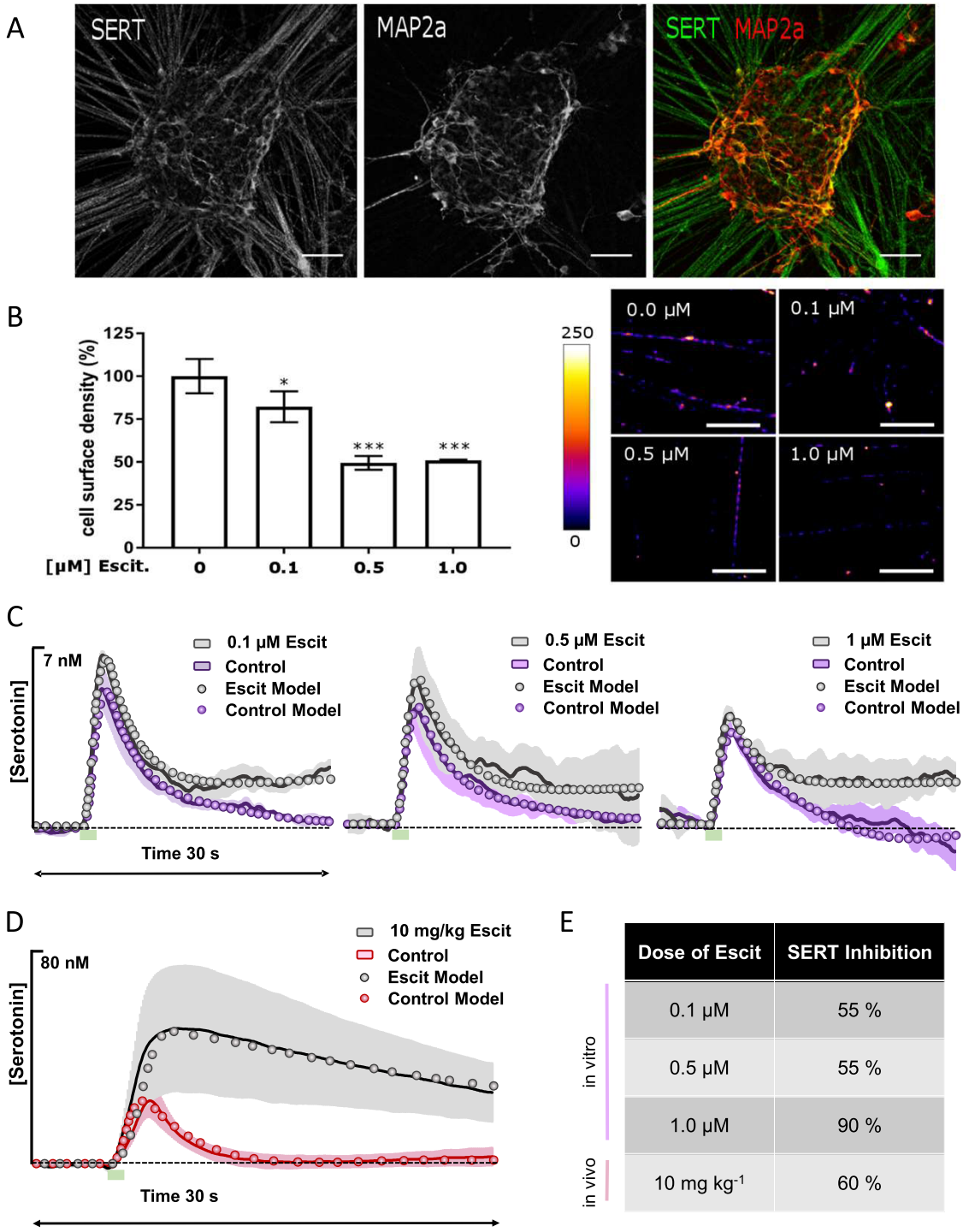

Dose of Escit	SERT Inhibition
0.1 μM	55 %
0.5 μM	55 %
1.0 μM	90 %
10 mg kg^{-1}	60 %

Figure 6. ESCIT-mediated SERT internalization. (A) Immunofluorescence analysis of 5-HTNs for SERT distribution. SERT signals can be found on Map2a-positive cell bodies and neurites as well as on Map2a-negative axons extending from the cluster. Scale bars: 50 μm. (B) Exemplary sum projections made from confocal stacks of ROIs acquired for SERT cell surface measurements. The Fire LUT bar (NIH ImageJ) indicates pixel intensities recorded on SERT-positive neurites ranging from 0 (black, no emission) to 255 (white, overexposed). Scale bars: 10 μm. After acute ESCIT exposure, SERT cell surface density significantly decreased for all concentrations tested (*$p < 0.05$ and *** $p < 0.001$ compared to the control neurons (0 μM ESCIT); 803 ROIs on neurites were quantified in three independent experiments). FSCV concentration vs time traces of serotonin reuptake: (C) Purple traces represent the control in different 5-HTN cultures; gray traces are after 0.1, 0.5, and 1 μM ESCIT exposure, respectively. Curves predicted by the mathematical model are superimposed with experimental data, represented with circular markers. (D) *In vivo* experiment showing serotonin release in the CA2 region of hippocampus in one cohort of mice (red) and again after 10 mg kg^{-1} (gray) ESCIT. Over each experimental trace are curves predicted by the model, represented with circular markers. The parameter choices and the information therein are discussed in the text. (E) The table reports the dose of ESCIT and the percent of SERT inhibition, as determined by the model.

from ESCIT-exposed cells fit 80% of control uptake for 0.1 μM, 50% of control uptake for 0.5 μM, and 50% of control uptake for 1 μM, representing 20, 50, and 50% inhibition of SERT-dependent serotonin uptake, respectively. These numbers are

https://doi.org/10.1021/acs.analchem.1c05082
Anal. Chem. XXXX, XXX, XXX−XXX

strikingly similar to the decrease in fluorescence intensity, validating the ability of our mathematical model to describe reuptake kinetics. Serotonin did not return to baseline and reached a new steady state in the presence of ESCIT after stimulation.

Data collected *in vivo* in the CA2 region of the hippocampus in a cohort of mice that received 1, 3, and 10 mg kg^{-1} ESCIT *i.p.* are shown in Figure S6A, with the 10 mg kg^{-1} dose shown in Figure 6D. These doses are roughly equivalent to the *in vitro* doses in Figure 6C.[22] This paradigm represents a well-established *in vivo* FSCV serotonin measurement experiment in a terminal area,[6] which does not necessarily represent the raphe-like nature of the 5-HTNs. Despite this, ESCIT caused an increase in the $t_{1/2}$ (time taken for the signal to clear to half maximum amplitude) of the serotonin clearance (9.0 ± 0.2 s control, 17.9 ± 1.1 s; 1 mg kg^{-1}, 22.1 ± 3.1 s; 3 mg kg^{-1}, 38.7 ± 7.3 s; 10 mg kg^{-1}). These data were also modeled (indicated by the dotted traces). We first chose parameters so that the computed extracellular serotonin curve matched the control. To fit the ESCIT curve 2 h after *i.p.* injection, the V_{max} of SERT fit was 80% of normal for 1 mg kg^{-1}, 60% of normal for 3 mg kg^{-1}, and 40% of normal for 10 mg kg^{-1}, representing 20, 40, and 60% SERT internalization, respectively (Figures 6D and S6B). These numbers are similar to those of the cells.

In previous studies, SSRIs induced concentration-dependent SERT internalization following SERT inhibition by SSRI.[21,23] Indeed, when we apply parameters for stronger SERT elimination, which reflect both inhibition and internalization of SERT, a specific SERT elimination of 55% for 0.1 μM, 55% for 0.5 μM, and 90% for 1 μM led to uptake curves that fit to the ESCIT-induced new steady-state levels in response to stimulation (Figure 6C,E).

DISCUSSION

5-HTNs Have *In Vivo*-Like Presynaptic Features. It is thought that *in vivo* serotonin release is *via* volume transmission.[24] Our characterization experiments present evidence for a distribution of presynaptic scaffolding proteins comparable to that of human dopaminergic *in vitro* neurons, which also perform volume transmission.[25] We also observed that SERT distribution in 5-HTNs is comparable to *in vivo* localization patterns in the rodent brain.[26] Furthermore, we demonstrate the uptake of synaptic vesicle dye by 5-HTNs. In line with these observations, release and reuptake of FFN511[27] and ASP+,[28] both fluorescent dyes for visualizing monoamine neurotransmission, occur along cell bodies and neurites. The application of ESCIT significantly reduced ASP+ uptake, indicating a predominantly SERT-driven uptake to which other monoamine transporters may contribute. Indeed, our RT-PCR analysis showed that 5-HTN cultures contain cells expressing DATs, NETs, and OCT3, which may also take up ASP+.[29,30] In summary, our fluorescence microscopy-based analysis implies that 5-HTNs perform extrasynaptic release of serotonin as observed *in vivo*. A recent study using aptamer-based sensors also measured serotonin release from cultured 5-HTNs.[31] More context can be provided for these findings by investigating *real-time* serotonin release and reuptake in 5-HTNs with a dynamic measurement model based on FSCV.

FSCV is a robust tool for chemical verification of neurotransmitters in dynamic systems[32] and has been used to study serotonin release from cells[33] and tissue slice preparations.[34,35] These models involved evoking transmitter release *via* electrical stimulation; thus, we adopted a similar approach by positioning a stimulating electrode around a cluster of cells. For the first time, we verify that 5-HTNs release and take up serotonin in real time in response to stimulation. This verification is *via* the characteristic position of redox peaks from FSCV color plots and CVs, previously found *in vivo*[36] and added here for comparison. Serotonin release from the 5-HTNs was lower than serotonin release found *in vivo* in mice. This finding explains the (seemingly) lower signal-to-noise ratio of cell signals compared to *in vivo* signals (larger error bars on cell data). The lower serotonin response in these cells is not surprising since we are probing a much less dense tissue area with an excess of electrolytic buffer surrounding the electrodes.

5-HTNs Are Neuro-Functionally Active. It is well established in the FSCV literature that stimulation strength influences the dynamics of neurotransmitter release.[37−41] 5-HTNs respond to stronger electrical stimulations by releasing more serotonin, showing that stimulation-sensitive excitatory mechanisms (found *in vivo*) for release are conserved in 5-HTNs.[37] Another important aspect for validating the functionality is the impact of precursor availability. For example, mast cells preloaded with TRP release more serotonin when stimulated,[33] and *in vivo* serotonin release can be induced from dopaminergic neurons by preloading with 5-hydroxytryptophan (5-HTP).[42] In accord with these studies, here, in 5-HTNs, serotonin release amplitude increased almost 2-fold (97.8%) by TRP preloading. This indicates that the 5-HTNs possess TRP-sensitive metabolic pathways (including tryptophan hydroxylase and 5-hydroxytryptophan decarboxylase), also verified *via* fluorescence staining of TPH2.

Multiple mechanisms for serotonin reuptake were first discussed by Shaskan and Snyder in 1970.[43] Since then, two classes of transporters have been identified that govern each uptake mechanism, Uptake 1 and Uptake 2 (*vide supra*). Previously, we provided *in vivo* FSCV evidence for these two reuptake mechanisms in different brain regions and utilized a model that contained two discrete Michaelis−Menten components to ascertain the contribution of each Uptake system to serotonin clearance.[7] Here, we use a similar approach to verify the presence of these two reuptake mechanisms in 5-HTNs. Here, we provide evidence of SERTs on 5-HTNs; thus, it is not surprising that our model captured the Uptake 1 processes. To investigate whether the same proteins that regulate Uptake 2 *in vivo* are responsible for the second uptake slope in 5-HTNs (DATs, NETs, and OCTs), we utilized RNA analysis. This analysis verified transcripts for DATs, NETs, and OCTs as found *in vivo* in serotonin terminal regions (on neurons and astrocytes). In the cultures utilized here, we cannot pinpoint the precise location of each transporter; however, it is likely that astrocytes are the primary source of non-SERT transporters.[44,45] Thus, in addition to *in vivo* serotonin release mechanisms being conserved in 5-HTN cultures, we now confirm that reuptake mechanisms are also conserved.

SSRI-Induced SERT Internalization: A Response Conserved between 5-HTNs and *In Vivo*. Previously, we employed murine serotonin neurons to investigate the role of allosteric SERT regulation in SSRI treatment and found that clinical doses of an established SSRI induced SERT internalization and that a mutated allosteric binding site led to stronger internalization effects.[21] A similar reduction in SERT function was previously postulated *in vivo*, as shown by reduced PET signals following the administration of ESCIT.[46] Here, under control conditions, SERTs were localized ubiquitously in 5-HTNs. As in our mouse model, acute ESCIT treatment induced

https://doi.org/10.1021/acs.analchem.1c05082
Anal. Chem. XXXX, XXX, XXX−XXX

dose-dependent internalization of SERTs (0.1, 0.5, and 1.0 μM). SERT internalization was also apparent in 5-HTNs *via* FSCV. Here, equivalent doses of ESCIT were perfused onto cell cultures and serotonin release was evoked. With all three doses, the serotonin released did not return to baseline. To mathematically model this data, we modified the original model, which required incorporation of a general internalization component (see eqs 1−5 in the Supporting Information). We extended this idea to the data collected *in vivo* in the mouse hippocampus after the mice were exposed to three doses of ESCIT *i.p.* and indeed found that the larger doses given *in vivo* necessitated incorporation of SERT internalization into the model. To our knowledge, this is the first time that SSRI-induced SERT internalization has been experimentally captured at such a rapid rate *in vivo*.

The *in vivo* experiment (measurement of terminal release in the hippocampus) is well established in our laboratory and does not mirror the raphe-like nature of the cultured 5-HTNs; however, even under these conditions, there are similarities between the models. A novel finding, *in vitro*, is that the signal after ESCIT does not return to baseline after stimulation, showing that a new steady state is reached. There could be a variety of explanations for this phenomenon, including a higher rate of ambient firing after stimulation and blockage of Uptake 2 transporters.[47,48] Here, the model captured this effect as further SERT internalization during stimulation. This effect is apparent to a lesser extent in the *in vivo* curves, likely because of the difference in how 5-HTNs are exposed to ESCIT. When ESCIT is added to the culture, it is done so as a rapid and consistent bolus, fundamentally different than an *i.p.* injection *in vivo*, where only a small fraction of ESCIT goes across the blood−brain barrier in a more diffuse concentration profile and is rapidly metabolized.[22,49] Similarly, the kinetics of reuptake differ between *in vivo* and 5-HTNs, which is likely due to the differences in the Uptake 1/Uptake 2 ratio between the systems. Nonetheless, the rapid internalization phenomenon is conserved between the models and implies that the mechanisms responsible for SERT internalization can act quickly, in accordance with recent evidence for rapid SERT shuttling between the cell surface and intracellular compartments.[50,51]

Another stark difference between the *in vitro* and *in vivo* data is the lack of increase in serotonin release amplitude after ESCIT *in vitro*. *In vivo*, the mechanisms governing this increased release have not been agreed upon. Given the lack of release increase *in vitro*, the implication here is that the nonserotonergic local environment *in vivo* (astrocytes, different neuronal types, mast cells, *etc.*) may contribute to the mechanism of the increased release. Thus, this *in vitro* model may also provide a platform for deciphering *in vivo* phenomena by simplifying the system.

We therefore provide evidence that our new voltammetric serotonin measurement model from human stem cell-derived 5-HTNs comprises key biochemical features of intact *in vivo* serotonin transmission. Our findings may provide a suitable representation of *in vivo* serotonin dynamics from a peripheral source, helping to bridge the translation between basic research in rodent models and humans toward advanced diagnostic and drug screening applications.

■ ASSOCIATED CONTENT

Supporting Information

The Supporting Information is available free of charge at https://pubs.acs.org/doi/10.1021/acs.analchem.1c05082.

Additional experimental details, materials, methods, and microscopy and voltammetry analyses (PDF)

■ AUTHOR INFORMATION

Corresponding Authors

Philipp Koch − *Department of Translational Brain Research, Central Institute of Mental Health, University of Heidelberg, Medical Faculty Mannheim, 68159 Mannheim, Germany; German Cancer Research Center, 69120 Heidelberg, Germany; HITBR Hector Institute for Translational Brain Research gGmbH, 68159 Mannheim, Germany*; Email: philipp.koch@zi-mannheim.de

Parastoo Hashemi − *Department of Chemistry and Biochemistry, University of South Carolina, Columbia, South Carolina 29208, United States; Department of Bioengineering, Imperial College London, London SW7 2AZ, U.K.*; orcid.org/0000-0002-0180-767X; Email: phashemi@imperial.ac.uk

Authors

Jordan Holmes − *Department of Chemistry and Biochemistry, University of South Carolina, Columbia, South Carolina 29208, United States*

Thorsten Lau − *Department of Translational Brain Research, Central Institute of Mental Health, University of Heidelberg, Medical Faculty Mannheim, 68159 Mannheim, Germany; German Cancer Research Center, 69120 Heidelberg, Germany; HITBR Hector Institute for Translational Brain Research gGmbH, 68159 Mannheim, Germany*

Rachel Saylor − *Department of Chemistry and Biochemistry, University of South Carolina, Columbia, South Carolina 29208, United States*

Nadine Fernández-Novel − *Department of Translational Brain Research, Central Institute of Mental Health, University of Heidelberg, Medical Faculty Mannheim, 68159 Mannheim, Germany; German Cancer Research Center, 69120 Heidelberg, Germany; HITBR Hector Institute for Translational Brain Research gGmbH, 68159 Mannheim, Germany*

Melinda Hersey − *Department of Chemistry and Biochemistry, University of South Carolina, Columbia, South Carolina 29208, United States; Department of Pharmacology, Physiology, & Neuroscience, University of South Carolina, Columbia, South Carolina 29209, United States*

Deanna Keen − *Department of Chemistry and Biochemistry, University of South Carolina, Columbia, South Carolina 29208, United States*; orcid.org/0000-0003-1513-5277

Lena Hampel − *Department of Translational Brain Research, Central Institute of Mental Health, University of Heidelberg, Medical Faculty Mannheim, 68159 Mannheim, Germany; German Cancer Research Center, 69120 Heidelberg, Germany; HITBR Hector Institute for Translational Brain Research gGmbH, 68159 Mannheim, Germany*

Sandra Horschitz − *Department of Translational Brain Research, Central Institute of Mental Health, University of Heidelberg, Medical Faculty Mannheim, 68159 Mannheim, Germany; German Cancer Research Center, 69120 Heidelberg, Germany; HITBR Hector Institute for Translational Brain Research gGmbH, 68159 Mannheim, Germany*

Julia Ladewig − *Department of Translational Brain Research, Central Institute of Mental Health, University of Heidelberg, Medical Faculty Mannheim, 68159 Mannheim, Germany;*

https://doi.org/10.1021/acs.analchem.1c05082
Anal. Chem. XXXX, XXX, XXX−XXX

German Cancer Research Center, 69120 Heidelberg, Germany; HITBR Hector Institute for Translational Brain Research gGmbH, 68159 Mannheim, Germany

Brenna Parke − *Department of Bioengineering, Imperial College London, London SW7 2AZ, U.K.*

Michael C. Reed − *Department of Mathematics, Duke University, Durham, North Carolina 27708, United States*

H. Frederik Nijhout − *Department of Biology, Duke University, Durham, North Carolina 27708, United States*

Janet Best − *Department of Mathematics, The Ohio State University, Columbus, Ohio 43210, United States*

Complete contact information is available at: https://pubs.acs.org/10.1021/acs.analchem.1c05082

Author Contributions

¶J.H. and T.L. contributed equally to the work.

Author Contributions

P.K., T.L., S.H., and J.L. developed and validated the cellular system and generated the cultures used in the cell culture experiments. J.H., P.H., R.S., and M.H. designed FSCV experiments. J.H., P.H., R.S., M.H., A.B., and D.K. performed FSCV experiments. J.H., P.H., M.L., and A.B. analyzed FSCV data. P.K. and T.L. designed the microscopy experiments. T.L., N.F.-N., and L.H. performed the microscopy experiments. T.L. performed STED microscopy. N.F.-N. and T.L. analyzed the microscopy data. M.C.R., N.F.H., and J.B. mathematically modeled the FSCV data. J.H., P.H., P.K., B.P., and T.L. wrote the manuscript.

Notes

The authors declare no competing financial interest.

■ ACKNOWLEDGMENTS

This work was funded by the National Institutes of Health R01MH106563 (PH) and the University of South Carolina Office of the Vice President for Research ASPIRE I Track IIB (RAS). JB was partially supported by the Mathematical Biosciences Institute at The Ohio State University through NSF Grant DMS-1440386. The authors would also like to acknowledge Colby Witt for contributing to the *in vivo* data collection, Navid Tavakoli for help with electrode fabrication, Isabell Moskal for excellent technical support, and Shane Berger for helpful conversations. The authors are very grateful to Janina Hanne, Hauke Kahl, and Jan-Gero Schlötel, Abberior Instruments (Göttingen, Germany), for making STED microscopy possible. The authors also acknowledge the generous financial support from the Hector Stiftung II.

■ REFERENCES

(1) Organization, W. H. *Depression*. https://www.who.int/news-room/fact-sheets/detail/depression (06/09/2021).
(2) Türközer, H. B.; Ongur, D. *Mol. Psychiatry* **2020**, *25*, 2214−2219.
(3) Hillhouse, T. M.; Porter, J. H. *Exp. Clin. Psychopharmacol.* **2015**, *23*, 1−21.
(4) Blackburn, T. P. *Pharmacol. Res. Perspect.* **2019**, *7*, No. e00472.
(5) Abdalla, A.; West, A.; Jin, Y.; Saylor, R. A.; Qiang, B.; Pena, E.; Linden, D. J.; Nijhout, H. F.; Reed, M. C.; Best, J.; Hashemi, P. *J. Neurochem.* **2020**, *153*, 33−50.
(6) Saylor, R. A.; Hersey, M.; West, A.; Buchanan, A. M.; Berger, S. N.; Nijhout, H. F.; Reed, M. C.; Best, J.; Hashemi, P. *Front. Neurosci.* **2019**, *13*, 362.
(7) Wood, K. M.; Zeqja, A.; Nijhout, H. F.; Reed, M. C.; Best, J.; Hashemi, P. *J. Neurochem.* **2014**, *130*, 351−359.
(8) West, A.; Best, J.; Abdalla, A.; Nijhout, H. F.; Reed, M.; Hashemi, P. *Neurochem. Int.* **2019**, *123*, 50−58.
(9) Abdalla, A.; Atcherley, C. W.; Pathirathna, P.; Samaranayake, S.; Qiang, B.; Pena, E.; Morgan, S. L.; Heien, M. L.; Hashemi, P. *Anal. Chem.* **2017**, *89*, 9703−9711.
(10) Wood, K. M.; Hashemi, P. *ACS Chem. Neurosci.* **2013**, *4*, 715−720.
(11) Hersey, M.; Samaranayake, S.; Berger, S. N.; Tavakoli, N.; Mena, S.; Nijhout, H. F.; Reed, M. C.; Best, J.; Blakely, R. D.; Reagan, L. P.; Hashemi, P. *J. Neurosci.* **2021**, *41*, 6564−6577.
(12) Hersey, M.; Woodruff, J. L.; Maxwell, N.; Sadek, A. T.; Bykalo, M. K.; Bain, I.; Grillo, C. A.; Piroli, G. G.; Hashemi, P.; Reagan, L. P. *Brain, Behav., Immun.* **2021**, *96*, 63−72.
(13) Soliman, M. A.; Aboharb, F.; Zeltner, N.; Studer, L. *Mol. Psychiatry* **2017**, *22*, 1241−1249.
(14) Brennand, K. J.; Simone, A.; Tran, N.; Gage, F. H. *Mol. Psychiatry* **2012**, *17*, 1239−1253.
(15) Hoffman, G. E.; Schrode, N.; Flaherty, E.; Brennand, K. J. *Mol. Psychiatry* **2019**, *24*, 49−66.
(16) Lu, J.; Zhong, X.; Liu, H.; Hao, L.; Huang, C. T.; Sherafat, M. A.; Jones, J.; Ayala, M.; Li, L.; Zhang, S. C. *Nat. Biotechnol.* **2016**, *34*, 89−94.
(17) Cao, L.; Hu, R.; Xu, T.; Zhang, Z. N.; Li, W.; Lu, J. *Front. Cell. Neurosci.* **2017**, *11*, No. 131.
(18) Gundelfinger, E. D.; Reissner, C.; Garner, C. C. *Front. Synaptic Neurosci.* **2015**, *7*, 19.
(19) Oz, M.; Libby, T.; Kivell, B.; Jaligam, V.; Ramamoorthy, S.; Shippenberg, T. S. *J. Neurochem.* **2010**, *114*, 1019−1029.
(20) Hashemi, P.; Walsh, P. L.; Guillot, T. S.; Gras-Najjar, J.; Takmakov, P.; Crews, F. T.; Wightman, R. M. *ACS Chem. Neurosci.* **2011**, *2*, 658−666.
(21) Matthäus, F.; Haddjeri, N.; Sanchez, C.; Marti, Y.; Bahri, S.; Rovera, R.; Schloss, P.; Lau, T. *Eur. Neuropsychopharmacol.* **2016**, *26*, 1806−1817.
(22) Sanchez, C.; Reines, E. H.; Montgomery, S. A. *Int. Clin. Psychopharmacol.* **2014**, *29*, 185−196.
(23) Benmansour, S.; Cecchi, M.; Morilak, D. A.; Gerhardt, G. A.; Javors, M. A.; Gould, G. G.; Frazer, A. *J. Neurosci.* **1999**, *19*, 10494−10501.
(24) Quentin, E.; Belmer, A.; Maroteaux, L. *Front. Neurosci.* **2018**, *12*, No. 982.
(25) Trueta, C.; De-Miguel, F. F. *Front. Physiol.* **2012**, *3*, 319.
(26) Liu, C.; Kershberg, L.; Wang, J.; Schneeberger, S.; Kaeser, P. S. *Cell* **2018**, *172*, 706−718 e15.
(27) Sur, C.; Betz, H.; Schloss, P. *Neuroscience* **1996**, *73*, 217−231.
(28) Baldinger, P.; Kranz, G. S.; Haeusler, D.; Savli, M.; Spies, M.; Philippe, C.; Hahn, A.; Hoflich, A.; Wadsak, W.; Mitterhauser, M.; Lanzenberger, R.; Kasper, S. *NeuroImage* **2014**, *88*, 252−262.
(29) Lau, T.; Proissl, V.; Ziegler, J.; Schloss, P. *J. Neurosci. Methods* **2015**, *241*, 10−17.
(30) Mason, J. N.; Farmer, H.; Tomlinson, I. D.; Schwartz, J. W.; Savchenko, V.; DeFelice, L. J.; Rosenthal, S. J.; Blakely, R. D. *J. Neurosci. Methods* **2005**, *143*, 3−25.
(31) Nakatsuka, N.; Heard, K. J.; Failletaz, A.; Momotenko, D.; Voros, J.; Gage, F. H.; Vadodaria, K. C. *Mol. Psychiatry* **2021**, *26*, 2753−2763.
(32) Ou, Y.; Buchanan, A. M.; Witt, C. E.; Hashemi, P. *Anal. Methods* **2019**, *11*, 2738−2755.
(33) Pihel, K.; Hsieh, S.; Jorgenson, J. W.; Wightman, R. M. *Biochemistry* **1998**, *37*, 1046−1052.
(34) Bunin, M. A.; Prioleau, C.; Mailman, R. B.; Wightman, R. M. *J. Neurochem.* **2002**, *70*, 1077−1087.
(35) John, C. E.; Jones, S. R. *Neuropharmacology* **2007**, *52*, 1596−1605.
(36) Hashemi, P.; Dankoski, E. C.; Petrovic, J.; Keithley, R. B.; Wightman, R. M. *Anal. Chem.* **2009**, *81*, 9462−9471.
(37) Hashemi, P.; Dankoski, E. C.; Lama, R.; Wood, K. M.; Takmakov, P.; Wightman, R. M. *Proc. Natl. Acad. Sci. U. S. A.* **2012**, *109*, 11510−11515.

(38) Wiedemann, D. J.; Garris, P. A.; Near, J. A.; Wightman, R. M. *J. Pharmacol. Exp. Ther.* **1992**, *261*, 574−579.
(39) Rice, M. E.; Cragg, S. J.; Greenfield, S. A. *J. Neurophysiol.* **1997**, *77*, 853−862.
(40) Threlfell, S.; Cragg, S. J.; Kallo, I.; Turi, G. F.; Coen, C. W.; Greenfield, S. A. *J. Neurosci.* **2004**, *24*, 8704−8710.
(41) Bunin, M. A.; Wightman, R. M. *J. Neurosci.* **1998**, *18*, 4854−4860.
(42) Stamford, J. A.; Kruk, Z. L.; Millar, J. *Brain Res.* **1990**, *515*, 173−180.
(43) Shaskan, E. G.; Snyder, S. H. *J. Pharmacol. Exp. Ther.* **1970**, *175*, 404−418.
(44) Furihata, T.; Anzai, N. *Biol. Pharm. Bull.* **2017**, *40*, 1153−1160.
(45) Takeda, H.; Inazu, M.; Matsumiya, T. *Naunyn-Schmiedeberg's Arch. Pharmacol.* **2002**, *366*, 620−623.
(46) Lundberg, J.; Christophersen, J. S.; Petersen, K. B.; Loft, H.; Halldin, C.; Farde, L. *Int. J. Neuropsychopharmacol.* **2007**, *10*, 777−785.
(47) Kita, J. M.; Parker, L. E.; Phillips, P. E.; Garris, P. A.; Wightman, R. M. *J. Neurochem.* **2007**, *102*, 1115−1124.
(48) Brennum, L.; Larsen, A.; Andesen, P.; Halldin, C. *Eur. Neuropsychopharmacol.* **2002**, *12*, 209.
(49) Bundgaard, C.; Eneberg, E.; Sanchez, C. *Neuropharmacology* **2016**, *103*, 104−111.
(50) Steiner, J. A.; Carneiro, A. M.; Blakely, R. D. *Traffic* **2008**, *9*, 1393−1402.
(51) Bermingham, D. P.; Blakely, R. D. *Pharmacol. Rev.* **2016**, *68*, 888−953.

https://doi.org/10.1021/acs.analchem.1c05082
Anal. Chem. XXXX, XXX, XXX−XXX